Targetable genetic signatures of immune evasion in lymphoma

Roemer, M.G.M.

2017

document version
Publisher's PDF, also known as Version of record

Chapter 2

Targetable genetic features of primary testicular and primary central nervous system lymphomas

Bjoern Chapuy,[1,*] Margaretha G.M. Roemer,[1,2,*] Chip Stewart,[3] Yuxiang Tan,[4] Ryan P. Abo,[5] Liye Zhang,[4] Andrew J. Dunford,[3] David M. Meredith,[6] Aaron R. Thorner,[5] Ekaterina S. Jordanova,[7] Gang Liu,[4] Friedrich Feuerhake,[8] Matthew D. Ducar,[5] Gerald Illerhaus,[9] Daniel Gusenleitner,[4] Erica A. Linden,[10] Heather H. Sun,[6] Heather Homer,[1] Miyuki Aono,[1] Geraldine S. Pinkus,[6] Azra H. Ligon,[6] Keith L. Ligon,[6] Judith A. Ferry,[11] Gordon J. Freeman,[1] Paul van Hummelen,[5] Todd R. Golub,[3,12] Gad Getz,[3,11] Scott J. Rodig,[6] Daphne de Jong,[2] Stefano Monti,[4] Margaret A. Shipp[1]

* Equal contribution

[1] Department of Medical Oncology, Dana-Farber Cancer Institute, Boston, MA, USA
[2] Department of Pathology, VU University Medical Center, Amsterdam, The Netherlands
[3] Broad Institute, Cambridge, MA, USA
[4] Section of Computational Biomedicine, Boston University School of Medicine, Boston, MA, USA
[5] Center for Cancer Genome Discovery, Dana-Farber Cancer Institute, Boston, MA, USA
[6] Department of Pathology, Brigham and Women's Hospital, Boston, MA, USA
[7] Center of Gynaecologic Oncology, VU University Medical Center, Amsterdam, The Netherlands
[8] Department of Pathology, Hannover Medical School, Hannover, Germany
[9] Department of Hematology and Oncology, University Hospital Freiburg, Freiburg, Germany
[10] Massachusetts General Hospital/North Shore Cancer Center, Danvers, MA, USA
[11] Department of Pathology, Massachusetts General Hospital, Boston, MA, USA
[12] Department of Pediatric Oncology, Dana-Farber Cancer Institute, Boston, MA, USA

Blood. 2016;127(7):869-881

Abstract

Primary central nervous system lymphomas (PCNSLs) and primary testicular lymphomas (PTLs) are extranodal large B-cell lymphomas (LBCLs) with inferior responses to current empiric treatment regimens. To identify targetable genetic features of PCNSL and PTL, we characterized their recurrent somatic mutations, chromosomal rearrangements, copy number alterations (CNAs), and associated driver genes, and compared these comprehensive genetic signatures to those of diffuse LBCL and primary mediastinal large B-cell lymphoma (PMBL). These studies identify unique combinations of genetic alterations in discrete LBCL subtypes and subtype-selective bases for targeted therapy. PCNSLs and PTLs frequently exhibit genomic instability, and near-uniform, often biallelic, *CDKN2A* loss with rare *TP53* mutations. PCNSLs and PTLs also use multiple genetic mechanisms to target key genes and pathways and exhibit near-uniform oncogenic Toll-like receptor signaling as a result of *MYD88* mutation and/or *NFKBIZ* amplification, frequent concurrent B-cell receptor pathway activation, and deregulation of BCL6. Of great interest, PCNSLs and PTLs also have frequent 9p24.1/*PD-L1*/*PD-L2* CNAs and additional translocations of these loci, structural bases of immune evasion that are shared with PMBL.

Key points:

- PCNSLs and PTLs have a defining genetic signature that differs from other LBCLs and suggests rational targeted therapies.
- PCNSLs and PTLs frequently exhibit 9p24.1/*PD-L1*/*PD-L2* copy number alterations and translocations, likely genetic bases of immune evasion.

Introduction

Diffuse large B-cell lymphomas (DLBCLs) often involve multiple nodal and extranodal sites. In contrast, large B-cell lymphoma (LBCL) subtypes, including primary central nervous system lymphoma (PCNSL), primary testicular lymphoma (PTL), and primary mediastinal large B-cell lymphoma (PMBL), present as localized masses in extranodal organs.[1-4] PCNSLs and PTLs, which both arise in sites that were previously considered to be immune sanctuaries, have inferior responses to therapies.[1-6] The defining genetic alterations in PCNSL and PTL and the relationships between these LBCLs, PMBL, and systemic DLBCL are incompletely characterized.

DLBCLs exhibit several types of low-frequency genetic alterations including copy number alterations (CNAs), mutations, and chromosomal rearrangements.[7] Certain alterations are more common in transcriptionally defined tumor subtypes. In the cell-of-origin classification, DLBCLs share transcriptional signatures of normal germinal center B-cells (GCBs) or in vitro activated B-cells (ABCs). ABC-type DLBCLs exhibit increased baseline NF-κB activity, more frequent genetic alterations of NF-κB and Toll-like receptor (TLR) signaling pathway components including mutations of *CARD11* and *MYD88* and the proximal B-cell receptor (BCR)-signaling pathway component, *CD79B*. However, these alterations are only detected in a subset of ABC-type DLBCLs (*MYD88*, 29%; *CD79B*, 18%; and *CARD11*, 10%).[8-10] Additional aspects of DLBCL heterogeneity are captured by the consensus clustering classification, which identifies "B-cell receptor," "Oxidative Phosphorylation," and "Host Response" subtypes.[11-13]

Recent genetic analyses of DLBCL underscore the importance of capturing both somatic mutations and CNAs.[14] Although only 15% to 20% of DLBCLs have inactivating *TP53* mutations, the majority of these tumors exhibit complementary CNAs that decrease p53 activity and perturb cell-cycle regulation.[14] DLBCLs with CNA-dependent p53 deficiency and cell-cycle deregulation have increased genomic instability and have a less favorable outcome.[14]

PMBL is a distinct LBCL subtype that exhibits constitutive NF-κB activation and shares certain clinical and genetic features with classical Hodgkin lymphoma (cHL).[15] We and others identified 9p24.1/*CD274(PD-L1)*/*PDCD1LG2(PD-L2)* copy gain, and increased expression of the PD-1 ligands in 65% of PMBLs.[16,17] Translocations of *PD-L1* and *PD-L2* were also reported in PMBL.[18,19] Genetic bases of PD-1 ligand overexpression are of particular interest given the role of PD-1 signaling in tumor-immune evasion and the efficacy of PD-1 blockade in other B-cell lymphomas with 9p24.1 copy gain.[20-22]

PCNSLs primarily arise in elderly patients and present as infiltrative masses of EBV^- tumor cells in periventricular white matter.[1,4] Additional EBV^+ PCNSLs occur in younger immunocompromised patients.[1] Reported CNAs include loss of the HLA-loci at 6p21.32 and deletion of *CDKN2A* in a minority of tumors.[5,23-25] Somatic mutations of *MYD88*, *CD79B*, and additional less common targets have been described.[23,24,26-28]

PTLs, which are the most common testicular tumors in elderly men,[2] present as focal masses with epididymal and scrotal involvement. At relapse, PTLs often involve additional extranodal sites including the central nervous system (CNS), skin, pleura, and contralateral testis. In previous array comparative genomic hybridization studies, PTLs exhibited frequent loss of the HLA-loci and 19q13 gain.[25] Somatic mutations of *MYD88* and *CD79B* of variable frequency have also been reported.[29,30]

Herein, we comprehensively characterize the genetic features of PCNSL and PTL and compare these tumors with systemic DLBCLs of known transcriptional subtypes and PMBL. The goal was to identify targetable lesions, bases of immune privilege in PCNSL and PTL, and unique combinations of genetic alterations in discrete LBCL subtypes.

Materials and Methods

Patients and primary tumor specimens

In accordance with local institutional review board protocols, newly diagnosed fresh-frozen PMBLs, EBV^- PCNSLs, and PTLs were obtained from Brigham and Women's Hospital, Massachusetts General Hospital, and University of Freiburg; formalin-fixed, paraffin-embedded (FFPE) PTLs and PCNSLs were obtained from the Netherlands Cancer Institute/VU University Medical Center Amsterdam and Brigham and Women's Hospital.

The discovery cohort includes the aforementioned primary LBCLs (PMBLs, PTLs, and PCNSLs with fresh-frozen tumor specimens) and an additional comparative cohort of previously analyzed primary DLBCL fresh-frozen biopsy specimens.[14] The number of discovery cohort samples analyzed for CNAs with high-density single nucleotide polymorphism (HD-SNP) arrays, transcript abundance with Affymetrix arrays, single-nucleotide variants (SNVs) with whole-exome sequencing (WES) of tumors and paired normals or RNA-Seq of tumors only and chromosomal rearrangement by DNA-Seq with a custom designed bait set are indicated in supplemental Figure 1A and supplemental Table 1A-B (available on the *Blood* Web site). An extension cohort of 43 PTLs, and 43 EBV^- and 8 EBV^+ PCNSLs from FFPE tissue were evaluated by quantitative polymerase chain reaction (qPCR) and

fluorescence in situ hybridization (FISH) for CNAs, qPCR and Sanger sequencing for SNVs, and immunohistochemical (IHC) analysis for protein expression as indicated in supplemental Figure 1B-C, supplemental Table 1C-D, and supplemental Methods. Supplemental Methods, Figures and Tables are available on the *Blood* Web site.

Results

Recurrent CNAs and candidate driver genes in LBCL subtypes

CNAs. To define recurrent CNAs in specific LBCL subtypes, we performed HD-SNP analyses of 21 EBV$^-$ PCNSLs, 7 PTLs, and 11 PMBLs and evaluated these data with the Genomic Identification of Significant Targets in Cancer (GISTIC) algorithm[31] (supplemental Figure 1 and supplemental Tables 1 and 2). Thereafter, we compared the recurrent CNAs in these LBCL subtypes with the previously described CNAs in 180 systemic DLBCLs[14] using mirror plots (Figure 1A-B and supplemental Figure 2). To quantify the relative frequencies of specific CNAs in the LBCL subtypes, we aggregated the HD-SNP array data from all LBCLs and applied the GISTIC algorithm (supplemental Table 3A-D). Subtype specific differences in the frequency of CNAs were assessed with an enrichment test (Figure 1C and supplemental Table 3E). Copy gains of 3q12.3, 18q21.33, and 19q13.42 and copy losses of 6p21.33, 6q21, and 9p21.3were significantly more frequent in PCNSL and PTL. Although the frequencies of 18q21.33 and 19q13.42 copy gain were comparable in PCNSL, PTL, and ABC-type DLBCLs, 9p21.3 copy loss was significantly more common and often biallelic in PCNSL and PTL (Figure 1C). Of interest, we found more frequent 9p24.1 copy gain in PTL, as in PMBL (Figure 1C).

Integrative analyses. To identify the genes perturbed by CNAs, we performed gene expression profiling on all LBCLs with available RNA and a representative subset of DLBCLs.[14] Genes within recurrent CNAs that had the most significant association between transcript abundance and copy gain or loss were defined as candidate drivers (supplemental Table 4).[14]

NFKBIZ, the candidate driver of 3q12.3 copy gain (Figure 1C), encodes IκB-ζ. This atypical IκB family member is induced by TLR signaling[32] and coactivates canonical and noncanonical NF-κB pathways.[32-34] 3q12.3/*NFKBIZ* copy gain was also detected in a subset of systemic DLBCLs (11% [19/180]) and a larger percentage of ABC type tumors (24% [13/55]) (Figure 1C and supplemental Figure 3).[14]

BCL2 was most closely associated with 18q21.33 copy gain, and *CDKN2A* was most tightly linked with 9p21.3 copy loss (Figure 1C); the peak of 6p21.33 copy loss included the *HLA-B* and *HLA-C* loci. PCNSL-selective 3p14.2 copy loss was associated with decreased expression of the tumor suppressor, FHIT (Figure 1C). In PTL, as in PMBL, 9p24.1 copy gain was linked with increased expression of the PD-1 ligand, PD-L2 (Figure 1C).

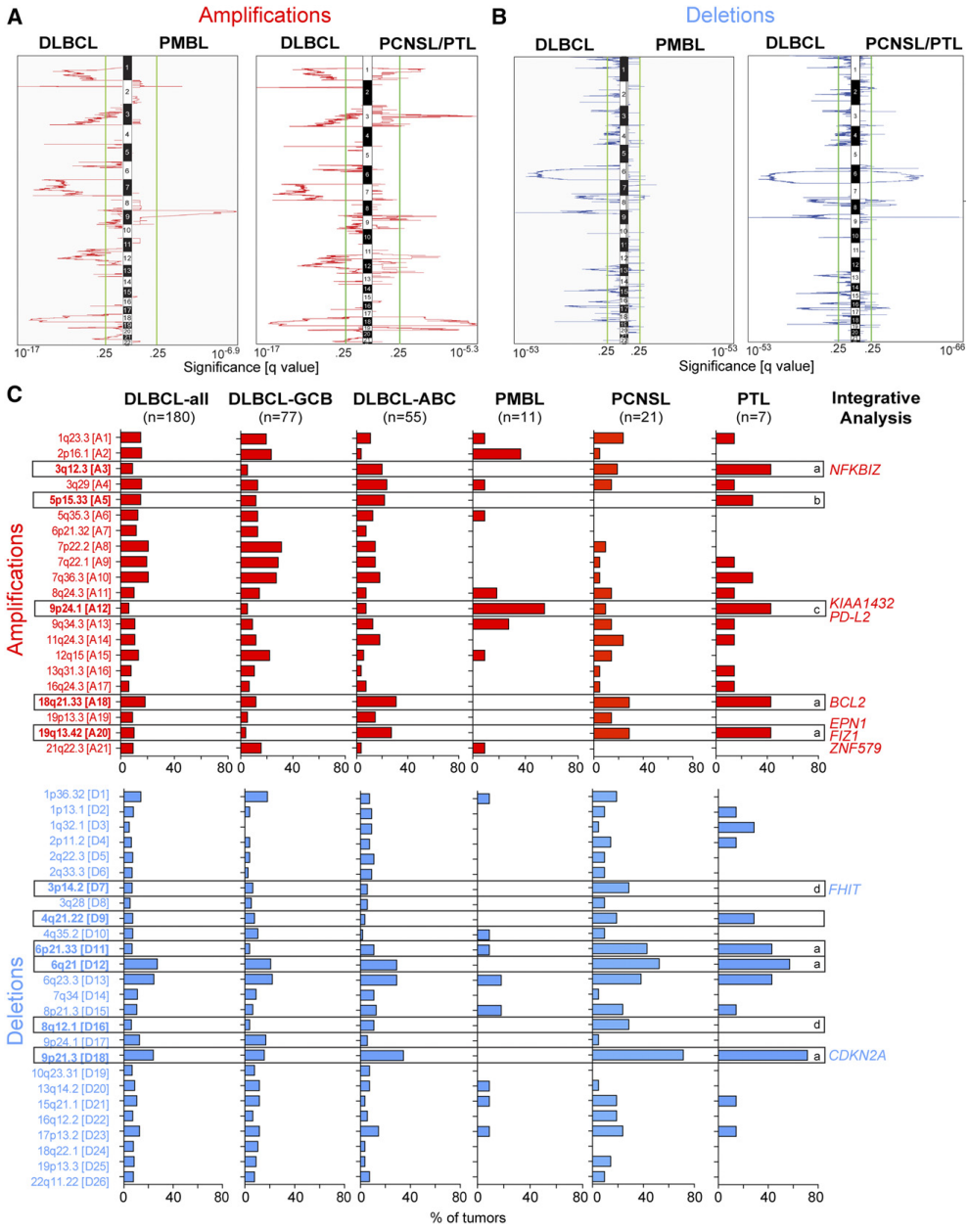

Figure 1. GISTIC-defined CNAs in LBCL subtypes. (A-B) GISTIC-defined recurrent CNAs (amplification in [A], red; deletions in [B], blue) in 180 primary DLBCLs[14] are compared with those in 11 PMBLs (left panel) and 28 PCNSLs/PTLs (right panel) in mirror plots. Chromosome position is on the y-axis, and significance is on the x-axis. The green line denotes q value of 0.25. (C) Frequencies of the 21 GISTIC-defined amplification peaks (top panel, red) and the 26 GISTIC-defined deletion peaks (bottom panel, blue) in the respective LBCL subtypes are plotted as bar graphs. DLBCL-GCB and DLBCL-ABC are subsets of DLBCL-All. CNAs that are more frequent in PTL and PCNSL (a), PTL only (b), PMBL and PTL (c), and PCNSL only (d), respectively, are noted. CNAs that are significantly enriched in PMBL, PCNSL, and/or PTL are boxed (FDR q value < 0.3; see also supplemental Table 2). Top genes by integrative analyses of copy number (CN) and transcript abundance are indicated on the right.

These data indicate that PCNSL and PTL share certain recurrent CNAs and candidate drivers that are also present in a subset of ABC-type DLBCLs. However, the defining CNA, 9p21.3/*CDKN2A* copy loss, was significantly more frequent in PCNSLs and PTLs than in ABC-type DLBCLs (71% [20/28] PCNSL/PTL vs 34.5% [19/55] ABC-type DLBCL; $P = .0023$; supplemental Table 3E). Furthermore, 9p21.3/*CDKN2A* copy loss was more often biallelic in PCNSL/PTL (50% [14/28] biallelic, 21% [6/28] monoallelic) compared with ABC-type DLBCLs (8% [5/62] biallelic, 26% [16/62] monoallelic; $P < .0001$).[14]

Patterns of CNAs and bases of genomic instability in LBCL subtypes

Certain DLBCLs have CNAs of multiple modulators of p53 activity and cell-cycle progression, increased genomic instability, and significantly higher total CNAs.[14] To evaluate patterns of CNAs in PCNSL, PTL, and PMBL, we performed unsupervised bihierarchical clustering. The majority of PCNSLs and PTLs were clustered together and characterized by frequent, often biallelic 9p21.3/*CDKN2A* loss and/or *FHIT* loss (branch I, Figure 2). These tumors also had increased genomic instability as reflected by significantly higher total CNAs (branch 1 vs branch 2; $P < .0001$). These findings likely reflect the complementary roles of the *CDNK2A* gene products, $p16^{INK4A}$ and $p19^{ARF}$, in p53 and cell-cycle regulation and the link between p53 deficiency, perturbed cell-cycle regulation, and genomic instability.[14,35-39] *FHIT* loss has also been associated with increased genomic instability.[40]

Almost all PMBLs (10/11), a small number of PCNSLs, and one PTL (4/28) were clustered in a branch with relatively few CNAs (branch II, Figure 2). In contrast to PMBLs, which exhibited 9p24.1/*PD-L2* copy gains with few other CNAs (branch II), PTLs and PCNSLs had 9p24.1/*PD-L2* copy gains in association with 9p21.3/*CDKN2A* copy loss and increased genomic instability (branch I, Figure 2).

Chromosomal rearrangements in PCNSL

We next assessed chromosomal rearrangements (including translocations, deletions duplications, and inversions) in 24 PCNSLs using a targeted DNA sequencing approach and a custom bait set covering 49 candidate genetic loci. The resulting data were analyzed with 2 complementary detection algorithms, dRanger/Breakpointer[41] and BreaKmer[42] (Figure 3A and supplemental Table 5A-C).

BCL6. The most frequent chromosomal rearrangements deregulated *BCL6* by juxtaposing the *IgH* super-enhancer[43] or 5'*HIST1H4I* regulatory elements to the *BCL6* 5'-untranslated region (5'UTR) (17% [4/24]) (Figure 3A and supplemental Figure 4). In 2 cases, deletions proximal to the 5'UTR of *BCL6* removed the regulatory elements, transcriptional start side, and first 5 exons of the *BCL6*-adjacent *LPP* gene

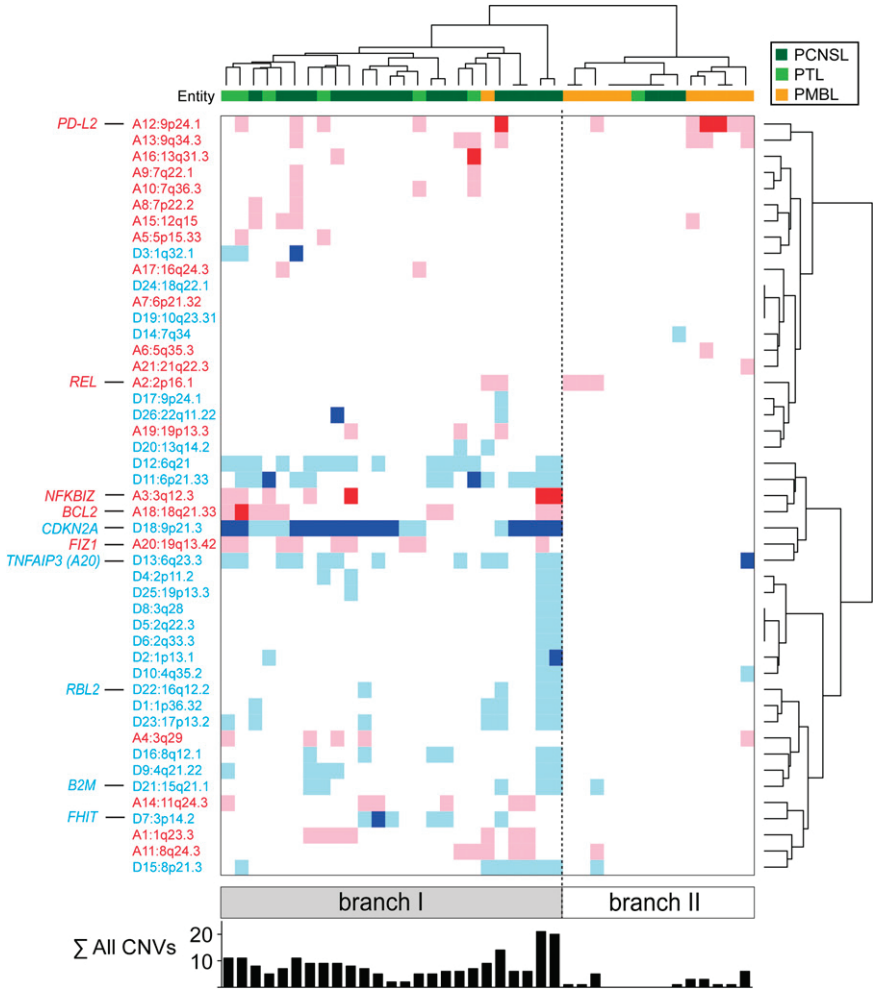

Figure 2. PCNSLs, PTLs, and PMBLs clustered by recurrent CNAs. (A) Unsupervised bihierarchical clustering of all 47 GISTIC-defined CNAs (y-axis) in 39 primary LBCLs (21 PCNSLs [dark green], 7 PTLs [light green], 11 PMBLs [orange]; x-axis). Copy gains, red; copy losses, blue; color intensity corresponds to magnitude of CNA. The sum of all GISTIC-defined CNAs per sample is listed below as a bar graph. Top genes by integrative analyses of CN and transcript abundance are indicated on the left.

(supplemental Figure 4C). This alteration may decrease the abundance of the *LPP*-intragenic miR-28, a reported tumor suppressor that is frequently downregulated in aggressive lymphomas.[44]

ETV6. Thirteen percent (3/24) of the PCNSLs had inactivating alterations of *ETV6*, deletions of exon 2 or exons 2-5 that altered the reading frame (Figure 3A and supplemental Figure 4B). *ETV6* encodes a transcriptional repressor perturbed by translocations, whole-gene deletions, or somatic mutations in multiple hematopoietic malignancies.[45] However, selective exon deletions that alter the *ETV6* reading frame were previously undescribed.

PD-L1/PD-L2. Of note, 13% (3/24) of PCNSLs had previously unidentified translocations involving the PD-1 ligand loci (Figure 3A). These included the juxtaposition of the *Igλ* super-enhancer proximal to the *PD-L2* 5'UTR or translocation of *BCNP1* (*FAM129C*)[46] regulatory elements proximal to the *PD-L1* start codon (Figure 3B and supplemental Figure 4). An additional PCNSL had an inactivating translocation of *CIITA*, the master transcription factor regulating MHC class II expression (Figure 3A).

Chromosomal rearrangements in PTL

Using the same approach, we analyzed chromosomal rearrangements in 7 PTLs from the discovery cohort.

BCL6. Two PTLs had translocations that deregulated BCL6-juxtaposition of the *Igλ* super-enhancer proximal to *BCL6* 5'UTR and the first reported translocation of the *Igκ* super-enhancer to the 5' regulatory elements of *PELI1* (Figure 3C and supplemental Figure 4A). *PELI1* encodes the E3 ubiquitin ligase, Pellino1, which stabilizes BCL6 via K63 polyubiquitination and promotes B-cell lymphomagenesis in a murine model.[47] As in PCNSL, one PTL had a deletion proximal to *BCL6* that removed the transcriptional start side and first 5 exons of *LPP* (supplemental Figure 4C).

ETV6. One PTL had an inactivating alteration of *ETV6* that disrupts the coding sequence (Figure 3C and supplemental Figure 4B).

PD-L2. Two PTLs had novel translocations involving *PD-L2*. In one case, the translocation juxtaposed the recently described *PAX5* super-enhancer[43] to the *PD-L2* 5'UTR (Figure 3C-D and supplemental Table 5C). In another, the translocation placed the 5' regulatory elements of *TBL1XL1* proximal to the first coding exon of *PD-L2* (Figure 3C-D and supplemental Figure 4E). These findings were confirmed using RNA-Seq and the QueryFuse algorithm[48] and a split-apart FISH assay (Figure 3E-F). The PTL with the *TBL1XR1-PD-L2* translocation also had increased PD-L2 expression (Figure 3G).

Recurrent somatic mutations in PCNSL

We next evaluated the PCNSLs for recurrent somatic mutations by performing WES on the subset of PCNSLs with available paired normal specimens (5 samples) and prioritizing the alterations with the MutSig2CV algorithm[49] (supplemental Figures 5 and 6 and supplemental Table 5D-F). To increase sample size, we performed RNA-Seq on an additional 9 PCNSLs and assessed the frequency of WES-detected mutations in the combined cohort (supplemental Table 5G-H). Eighty-six percent (12/14) of the analyzed PCNSLs exhibited oncogenic gain-of-function mutations in *MYD88* (*MYD88*^{L265P}); 64%(9/14) had missense mutations in the immunoreceptor

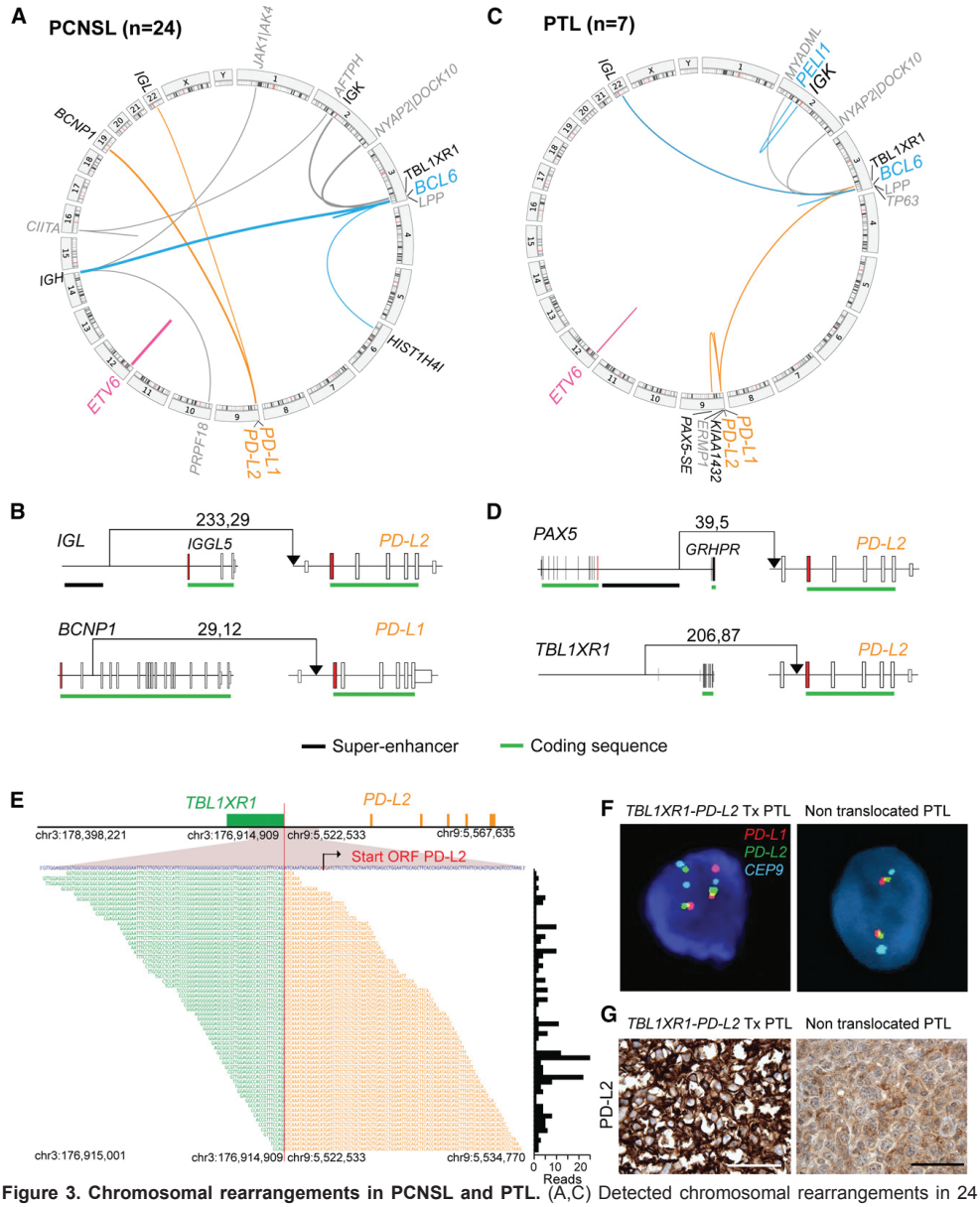

Figure 3. Chromosomal rearrangements in PCNSL and PTL. (A,C) Detected chromosomal rearrangements in 24 PCNSL (A) and 7 PTL (C) are summarized as circos plots. Structural alterations involving certain partners are highlighted; *BCL6*, blue; *ETV6*, pink; PD-1 ligands, orange. Partners of color-coded alterations are black, all other alterations are gray. Frequency of events is indicated by line thickness. (B,D) Chromosomal rearrangements involving *PD-L1* or *PD-L2* are plotted in their genomic context. Exons are visualized as boxes, ATG-containing exon are in red, the coding region is underlined in green, and previously identified super-enhancers in DLBCLs[43] are underlined in black. The number of supporting reads (split reads, read pairs) is indicated above each translocation. (E) *TBL1XR1-PD-L2* fusion as validated by RNA-Seq. Chromosomal breakpoint is depicted by the red line. Start codon of *PD-L2* is indicated in red within the contig of the RNA-Seq reads. The translocation involves only the regulatory elements of *TBL1XR1* and does not affect the open reading frame (ORF) of *PD-L2*. Individual supporting reads are shown in the lower panel, with frequencies as a bar graph on the right. (F) FISH assays of PTLs with the *PD-L2* translocation (left panel) or with wild-type *PD-L2* (right panel). *PD-L1* in red, *PD-L2* in green, and centromeric probe (CEP9) in aqua. (G) IHC of PD-L2 expression in the translocated PTL (left panel) and a PTL with wild-type *PD-L2* (right panel). The scale bar represents 100 µm.

tyrosine-based activation motif domain of *CD79B* and 29% (4/14) had missense mutations in the coiled-coil domain of *CARD11* (Figure 4A and supplemental Figure 7). These data indicate that canonical *MYD88* and *CD79B* mutations are more frequent in PCNSLs than in previously reported ABC-type DLBCLs (*MYD88*, 29%[8]; *CD79B*, 18%[9]).

PCNSLs also exhibited frequent (71%[10/14]) missense mutations in the kinase domain of *PIM1*, a known target of aberrant somatic hypermutation (Figure 4A and supplemental Figure 7D). In addition, 29% (4/14) of the evaluated PCNSLs had mutations in *IRF4*. The encoded IRF4 transcription factor, which regulates germinal center exit, class switch recombination, and plasma cell development is also expressed in ABC-type DLBCLs (Figure 4A and supplemental Figure 7).[50]

Twenty-one percent (3/14) of PCNSLs exhibited mutations of *ETV6* (Figure 4A and supplemental Figure 7D), which was also perturbed by inactivating deletions of coding exons (Figure 3A and supplemental Figure 4). PCNSLs also had mutations of *BTG1* (43% [6/14]) and *TBL1XR1* (36% [5/14]), transcriptional cofactors that regulate ETV6 activity (Figure 4A and supplemental Figure 7D).[51] Of interest, TBL1XR1 also modulates TLR/MYD88 signaling by increasing clearance of NCor/SMRT transcriptional corepressors from certain TLR/MYD88 target genes.[52]

Patterns of genetic alterations in PCNSLs

After defining recurrent mutations, chromosomal rearrangements, and CNAs in PCNSL, we assessed the patterns of alterations in individual tumors. Mutations and CNAs that occurred in ≥20% (3/14) of tumors were included and chromosomal rearrangements were added (Figure 4B). In these PCNSLs, all *CD79B* mutations occurred in the context of *MYD88* mutations. Similarly, the less frequent *CARD11* mutations all occurred in *MYD88* mutation-positive PCNSLs, three of which had concurrent *CD79B* mutations. PCNSLs with copy loss of *TNFAIP3* also had concurrent *CD79B* and *MYD88* mutations. In the analyzed PCNSLs, *MYD88* mutations also occurred in association with additional potential modulators of TLR signaling such as *NFKBIZ* copy gains (Figure 4B). Furthermore, these PCNSLs often had mutations and/or exon deletions of *ETV6*, and/or mutations of the transcriptional cofactors *BTG1* and *TBL1XR1*.

The majority of PCNSLs also had evidence of genomic instability as reflected by *CDKN2A* and/or *FHIT* loss and multiple additional CNAs (Figure 2 and 4B). However, PCNSLs had infrequent *TP53* mutations (7% [1/14]), likely because *CDKN2A* deregulates the same pathway upstream of *TP53*.[14,53]

Recurrent mutations in PTL

Given the shared genetic features of PCNSL and PTL (Figures 1-3), we next evaluated the spectrum of mutations in the series of available PTLs. In the absence of paired germline DNA samples, we performed RNA-Seq on 6 PTLs and identified SNVs after filtering out known SNPs (Figure 4C and supplemental Table 5I). In these PTLs, we focused on genes that were mutated in our WES PCNSL cohort or systemic DLBCLs, or those that were previously deposited in the COSMIC database.[54-58] Like the PCNSLs, the PTLs had frequent *CD79B* and *MYD88* mutations and additional mutations of *PIM1* and *BTG1* (Figure 4C). Mutations of *MEF2B*, a transcriptional activator and regulator of BCL6 expression,[59] were also identified (Figure 4C and supplemental Figure 7D). *MEF2B* alterations were previously reported in ~8% of systemic DLBCLs of the ABC and GCB subtypes.[59]

Patterns of genetic alterations in PTL

As in the PCNSLs, *CD79B* and *MYD88* mutations were largely concurrent in the PTLs; *PIM1*, *BTG1*, and *MEF2B* alterations were detected within this subset of *CD79B*/*MYD88*-mutated tumors (Figure 4D). The aforementioned mutations occurred in the setting of frequent, often biallelic, *CDKN2A* copy loss, *TNFAIP3* copy loss, and *NFKBIZ* copy gain. In addition, PTLs had multiple bases of deregulating BCL6 including mutations of *MEF2B* and translocations of *Igλ-PELI1* (Figure 4D) and *Igλ-BCL6* (Figure 3C).

Validation of recurrent CNAs in a PTL extension cohort

Given the small size of our discovery PTL cohort, we obtained an additional 43 FFPE PTLs to evaluate specific recurrent CNAs and SNVs (supplemental Figure 8 and supplemental Table 1C-D). We established qPCR assays for the most significant CNAs/driver genes using DNA from informative LBCL cell lines and normal lymphoid cells as controls (supplemental Table 6). *CDKN2A* integrity was assessed with 3 independent probe sets that covered exons coding for $p16^{INK4A}$ and $p19^{ARF}$ (supplemental Figure 8A-B). Mono- or biallelic loss of the full *CDKN2A* locus was detected in ~81%(35/43) of tumors (supplemental Figure 8A). Frequent copy gain of 18q21.33/*BCL2* (47% [20/43]) and 19q13.42/*FIZ1* (70% [30/43]) were also confirmed (supplemental Figure 8C-D).

Functional consequences of 3q12.3/*NFKBIZ* copy gain and near-uniform oncogenic TLR signaling in PTL and PCNSL

In the PTL extension cohort, 44% of these tumors also had 3q12.3/*NFKBIZ* copy gain (Figure 5A, left panel). Similar to the PTL discovery cohort (Figure 4C), 79% (34/43) of the PTL extension series had $MYD88^{L265P}$ mutations (Figure 5B, left

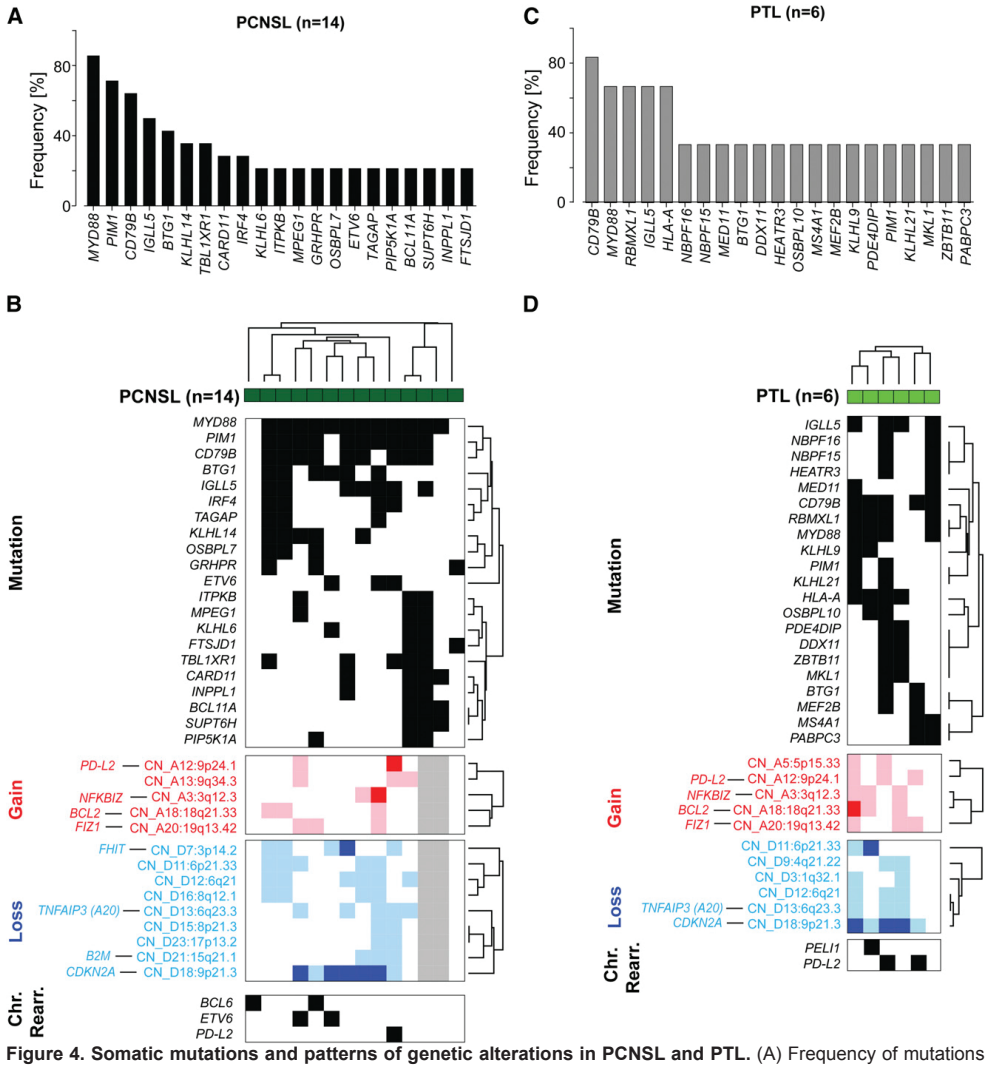

Figure 4. Somatic mutations and patterns of genetic alterations in PCNSL and PTL. (A) Frequency of mutations in PCNSLs (mutations initially identified by WES in 5 tumor/normal pairs and subsequently assessed in 9 additional tumors without paired normals by RNA-Seq). See also supplemental Table 5D-H. Only genes mutated in at least 20% (3 patients) are shown. (B) Mutations occurring in at least 20% (3/14) of PCNSL samples (dark green) are plotted in a black-and-white–coded matrix (x-axis, samples; y-axis, mutations; black, mutation present; white, mutation absent) and clustered bihierarchically. CNAs in these PCNSLs are visualized as a color-coded heat map below; copy gain, red; copy loss, blue; not available, gray; color intensity corresponds to magnitude of CNA. Top genes by integrative analyses of CN and transcript abundance are indicated on the left, y-axis. Chromosomal rearrangements of *BCL6*, *ETV6*, or *PD-L2* are added below. (C) Frequency of mutations in 6 PTLs as assessed by RNA-Seq. Only mutations present in at least 2 patients are shown (supplemental Table 5I, full list). SNVs were filtered for known SNPs; only SNVs previously deposited in COSMIC or reported to be mutated in DLBCLs/PCNSLs are shown. (D) Mutations present in at least 2 PTLs (y-axis) are plotted in a black-and-white–coded matrix as in (B) and clustered bihierarchically. CNAs in these PTLs are visualized as a color-coded heat map below, and selected chromosomal rearrangements modifying BCL6 (*PELI1*) and *PD-L2* are added at the bottom.

panel, and supplemental Table 6A). Thirty-eight percent (13/34) of PTLs with *MYD88* mutations also had *NFKBIZ* copy gains; in addition, 5 of 9 tumors with wild-type *MYD88* had *NFKBIZ* copy gains (Figure 5B, left panel).

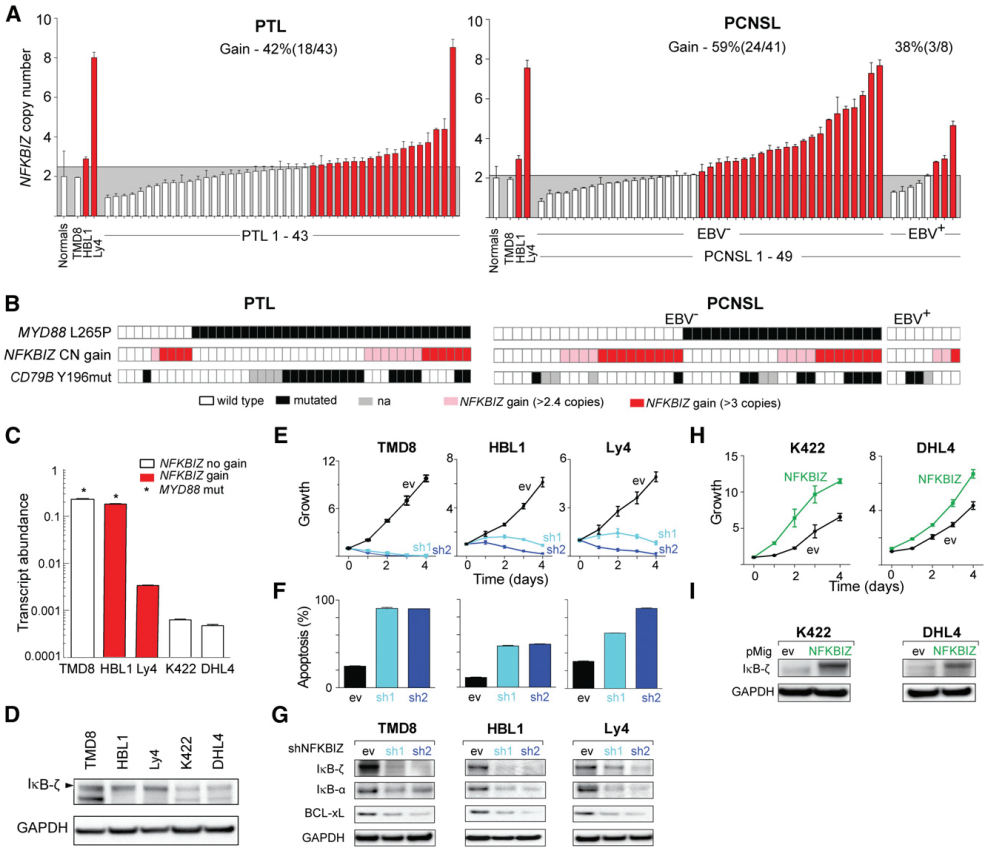

Figure 5. Functional consequences of 3q12.3/*NFKBIZ* copy gain and IκB-ζ overexpression. (A) CN of 3q12.3/*NFKBIZ* in 43 PTLs (left panel) and 49 PCNSLs (41 EBV⁻ and 8 EBV⁺, right panel) from the extension cohorts. Normals include 5 tonsils and 5 reactive lymph nodes. The upper 95% confidence interval of the normals was used as a threshold for copy gain. Indicated cell lines with known *NFKBIZ* CNs were used as controls. Cases with copy gain are shown in red. Error bars reflect standard deviation. (B) Cosegregation of genetic alterations in the TLR pathway (*MYD88* mutations [upper panel; black, L265P; white, no L265P], *NFKBIZ* copy gain [middle panel; copy gain, red; color intensity corresponds to magnitude of copy gain]) and BCR pathway (*CD79B* mutations [lower panel; black, missense mutations affecting Y196; white, no exon 5 mutations; gray, not available]) in the 43 PTL samples (left panel), and 49 PCNSL cases (right panel; 41 EBV⁻ and 8 EBV⁺). (C) IκB-ζ encoded by *NFKBIZ* locus transcript abundance in representative DLBCL cell lines. Asterisks indicate cell lines with *MYD88*^{L265P} mutation. (D) IκB-ζ protein abundance in indicated cell lines. Full-length IκB-ζ is indicated with an arrowhead. Note that TMD8 has a heterozygous deletion of 159 base pairs, resulting in a shorter, fully functional IκB-ζ protein.[32] The membrane was reprobed for glyceraldehyde-3-phosphate dehydrogenase (GAPDH) as loading control. (E-F) Proliferation (E) and apoptosis (F) after knockdown of IκB-ζ (sh1 and sh2, 2 independent IκB-ζ hairpins; ev, control) in representative DLBCL cell lines with increased IκB-ζ transcript abundance resulting from *NFKBIZ* gain only (Ly4), *MYD88* mutation only (TMD8), or both (HBL1). (G) Efficacy of knockdown of IκB-ζ and downstream targets was determined by immunoblot. (H) Proliferation after enforced expression of IκB-ζ in cell lines with low IκB-ζ transcript levels (DHL4 and K422). (I) Efficacy of IκB-ζ overexpression was determined by immunoblot.

We also assessed the 3q12.3/*NFKBIZ* locus in an extension cohort of PCNSLs including 41 EBV⁻ and 8 EBV⁺ tumors; 59% (24/41) of EBV⁻ PCNSLs and 38%(3/8) of EBV⁺ PCNSLs had 3q12.3/*NFKBIZ* copy gain (Figure 5A, right panel). In the EBV⁻ PCNSL extension cohort, 83% of tumors had 3q12.3/*NFKBIZ* copy gain, *MYD88*^{L265P} mutations, or both alterations (Figure 5B, right panel). Interestingly, none of the 8

EBV^{+} PCNSL cases had an oncogenic *MYD88*^{L265P} mutation. Taken together, these data suggest that *NFKBIZ* copy gain or viral infection may serve as additional and/or alternative oncogenic modulators of the MYD88/TLR signaling pathway.

We next assessed the functional consequences of *NFKBIZ* copy gain using a panel of informative LBCL cell lines with known *NFKBIZ* CN and *MYD88* mutational status (Figure 5C). Cell lines with wild-type *MYD88* and no *NFKBIZ* copy gain (K422, DHL4) had the lowest IκB-ζ transcript and protein levels, whereas cell lines with *MYD88* mutation alone (TMD8), *MYD88* mutation, and *NFKBIZ* copy gain (HBL1), or *NFKBIZ* copy gain alone, (Ly4) had more abundant IκB-ζ transcripts and protein (Figure 5C-D). In the 3 LBCL cell lines with high baseline IκB-ζ expression (TMD8, HBL1, Ly4), IκB-ζ depletion significantly decreased cellular proliferation, induced apoptosis, and reduced expression of the IκB-ζ target genes, IκB-α and BCL-xL (Figure 5E-G).[32] In LBCL cell lines with low baseline IκB-ζ transcript levels (K422, DHL4), enforced expression of IκB-ζ conferred a growth advantage (Figure 5H-I). These genetic and functional analyses define *NFKBIZ* copy gain as an alternative oncogenic TLR signaling mechanism in LBCL.

Concurrent alterations of TLR and BCR signaling pathway components in PTL and PCNSL

Recent data suggest that TLR/MYD88 activation may directly augment BCR-mediated survival signals[60,61] in addition to modulating NF-κB. The frequent co-occurrence of *MYD88* and *CD79B* mutations in the initial PTL and EBV^{-} PCNSL series (Figure 4B,D) prompted us to evaluate *CD79B* hotspot mutations in both extension cohorts. Forty-four percent (17/39) of evaluable PTLs had *CD79B*^{Y196} mutations, almost all (16/17) of which occurred in tumors with *MYD88*^{L265P} alterations (Figure 5B, left panel). In the extension cohort of EBV^{-} PCNSLs, 28% (10/36) had *CD79B*^{Y196} mutations, 80% (8/10) in association with *MYD88*^{L265P} (Figure 5B, right panel). Both EBV^{-} PCNSLs and PTLs were significantly more likely to have co-occurring *CD79B* and *MYD88* mutations than systemic DLBCLs or the ABC DLBCL subset (supplemental Table 6C).

9p24.1 copy gain and PD-1 ligand expression in PTL and PCNSL

A shared genetic feature of PMBLs and the PTL discovery cohort was frequent 9p24.1 copy gain; several EBV^{-} PCNSLs also had this alteration (Figure 1). PTLs in the extension cohort also exhibited frequent 9p24.1/*PD-L1*/*PD-L2* copy gain by ligand-specific qPCR (Figure 6A-B) and CN-associated expression of these ligands by IHC (Figure 6C-D). Using tissue microarrays of the same PTLs, we also identified tumor-infiltrating T cells that expressed the PD-1 receptor (supplemental Figure 9A-B).

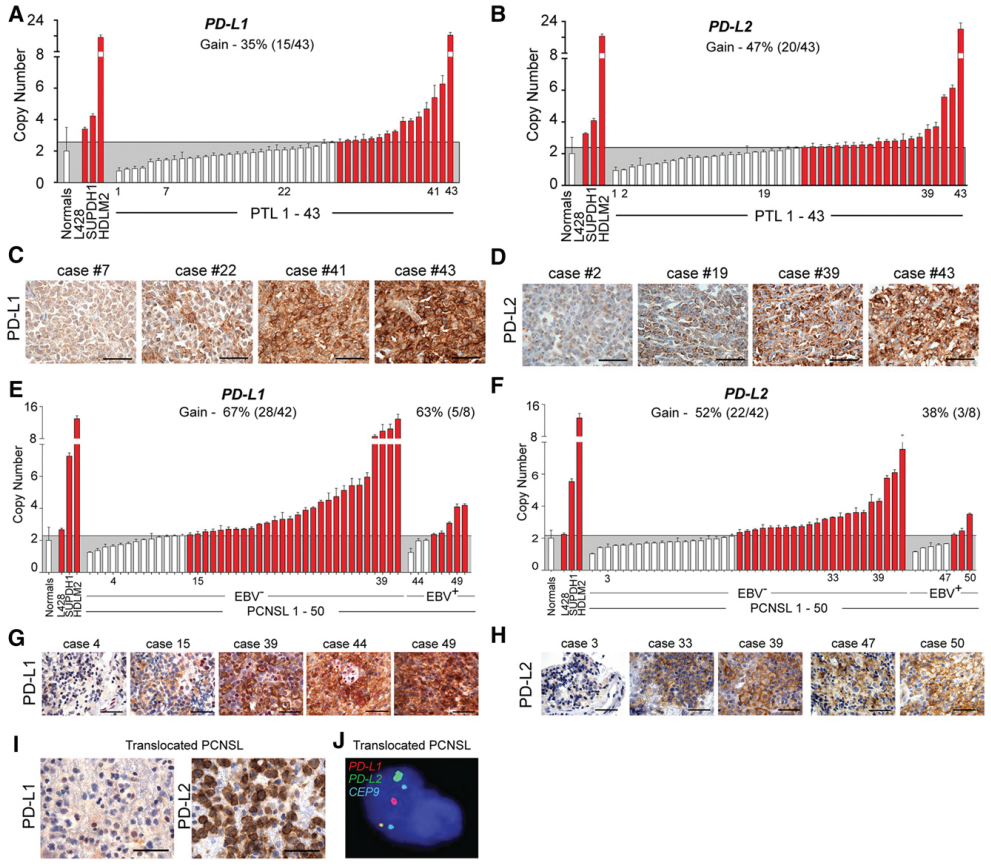

Figure 6. Genetic alterations of *PD-L1* and *PD-L2* in PTL and PCNSL. (A) CNs of *PD-L1* in 43 PTL cases from the extension cohort. Normals include 5 tonsils and 5 reactive lymph nodes. The upper 95% confidence interval of the normals was used as a threshold for CN gain in the PTLs. Indicated cHL cell lines with known *PD-L1* copy gain were used as controls. Cases with copy gain are highlighted in red. Error bars reflect standard deviation. (C) PD-L1 protein expression in indicated cases from (A). The scale bar represents 100 µm. (B) CNs of *PD-L2* in 43 PTL cases from extension cohort. Controls are as in (A). (D) PD-L2 protein expression in indicated cases from (B). (E) CNs of *PD-L1* in 50 PCSNL cases (42 EBV$^-$ and 8 EBV$^+$) from the extension cohort. Details are as in (A). (F) CNs of *PD-L2* in 50 PCSNL cases (42 EBV$^-$ and 8 EBV$^+$) from extension cohort. Controls are as in (A). (G) PD-L1 protein expression in indicated cases from (E). The scale bar represents 100 µm. (H) PD-L2 protein expression in indicated cases from (F). (I) PD-L1 (left panel) and PD-L2 (right panel) of the PCNSL case with wild-type *PD-L1/2* CN. (J) Split-apart FISH assay of the PCNSL in (I). *PD-L1* in red, *PD-L2* in green and centromeric probe (CEP9) in aqua.

Bases of PD-1 ligand deregulation in PCNSL

We similarly evaluated the *PD-L1*/*PD-L2* loci in the extension cohort of 42 EBV$^-$ PCNSLs and 8 EBV$^+$ PCNSLs. In the larger EBV$^-$ PCNSL series, the majority of tumors exhibited 9p24.1/*PD-L1*/*PD-L2* copy gain (67% [28/42]) and CN-associated increased expression of these ligands (Figure 6E-H). We also identified a copy-neutral case with discordant low-level PD-L1 and high-level PD-L2 protein expression and used the split-apart *PD-L1*/*PD-L2* FISH assay to detect a chromosomal rearrangement that selectively deregulated PD-L2 (Figure 6I-J).

In the EBV$^+$ PCNSLs, we noted largely CN-independent high-level expression of PD-L1 and PD-L2[16,62,63] (Figure 6E-H). Compared with EBV$^-$ PCNSLs, EBV$^+$ tumors had lower-level *PD-L1*/*PD-L2* copy gain, consistent with an additional viral mechanism of PD-1 ligand upregulation in these tumors (Figure 6E-F).

These data extend the molecular similarities in PCNSL and PTL to include 2 genetic bases of PD-1 ligand overexpression, copy gain, and chromosomal translocation, and implicate EBV infection as an additional mechanism of PD-1 ligand upregulation in PCNSLs.

Discussion

We have defined recurrent mutations, chromosomal rearrangements, CNAs, and associated driver genes in PCNSL and PTL and compared these comprehensive genetic signatures with those of systemic DLBCL and PMBL. These analyses revealed new genetic features, unique combinations of alterations, and a distinctive signature of near-uniform oncogenic TLR signaling with frequent concurrent BCR activation and genomic instability in PCNSL and PTL (Figure 7). The studies also identified specific genetic bases of deregulated PD-1 ligand expression and likely immune evasion in PCNSL and PTL (Figure 7). Most importantly, several of these genetic alterations are amenable to targeted therapy.

Incidence and bases of genomic instability in the LBCL subtypes

Comparative analyses of CNAs in the LBCL subtypes revealed distinct differences in incidence and bases of genomic instability in these lymphomas. In contrast to the majority of systemic DLBCLs, PCNSLs, and PTLs, PMBLs have relatively few CNAs (Figure 7). The paucity of CNAs, other than 2p16.1 and 9p24.1 copy gain, distinguish PMBLs from the additional evaluated LBCLs. PMBLs also lack genetic alterations known to either induce or tolerate genomic instability including CNAs of *CDKN2A*, *RB1*, or *TP53* (Figure 7).[14,35-39]

Our analyses further suggest that systemic DLBCLs, PCNSLs, and PTLs use different mechanisms to tolerate or induce genomic instability. Systemic DLBCLs primarily exhibit genomic instability in the setting of multiple low-frequency CNAs of p53/cell-cycle components and additional *TP53* somatic mutations (Figure 7).[14] In contrast, PCNSLs and PTLs rarely have *TP53* mutations but frequently perturb the p53 pathway via upstream, often biallelic, *CDKN2A* loss (Figure 7). As a consequence, PCNSLs and PTLs may be candidates for MDM2/4 inhibitors that augment wild-type p53 activity[64] and CDK-blockade.[14]

Near-uniform oncogenic TLR signaling in PCNSL and PTL

We found oncogenic *MYD88*^{L265P} mutations and/or *NFKBIZ* copy gain to be near-universal genetic features of EBV^{-} PCNSL and PTL; both alterations were significantly more common in these lymphomas than in ABC-type DLBCLs (Figure 7).[8] IκB-ζ transcription is induced by *MYD88* mutations[32] or *NFKBIZ* amplification, and IκB-ζ depletion is lethal in each setting, suggesting that IκB-ζ is an essential intermediary in oncogenic TLR signaling. *NFKBIZ* copy gain also represents an alternative and/or complementary structural basis for increased TLR activity in PTL and PCNSL (Figure 7).

Genetic alterations that complement oncogenic TLR signaling in PCNSL and PTL

Recent murine studies suggest that the consequences of enforced *MYD88*^{L265P} expression in normal B cells depend on additional complementary genetic alterations.[65] Although *MYD88*^{L265P} increased cellular proliferation and activated NF-κB in antigen-exposed murine B cells, these effects were rapidly countered by TNFAIP3 induction and BIM-dependent apoptosis.[65] In this model, *TNFAIP3* inactivation or enforced BCL2 expression was required to sustain *MYD88*^{L265P}-dependent signaling.[65] These findings are of particular interest because PCNSLs and PTLs frequently exhibit *TNFAIP3* copy loss and/or *BCL2* copy gain in association with *MYD88*^{L265P} and/or *NFKBIZ* copy gain (Figure 4). The identification of these complementary genetic alterations required concurrent analyses of mutations, CNAs, and associated driver genes.

Concurrent oncogenic TLR signaling and BCR activation in PCNSL and PTL

In our series of PCNSLs and PTLs, *CD79B* mutations primarily occurred in the context of oncogenic TLR signaling. The high incidence of concurrent *CD79B* and *MYD88* mutations is an additional distinguishing feature of PCNSLs and PTLs compared with the more heterogeneous group of ABC-type DLBCLs (Figure 7). Given the near-universal genetic alterations of TLR and BCR signaling in PCNSL and PTL, these tumors may be particularly vulnerable to targeted inhibition of pathway components such as IRAK1/4, IRF4, and/or BTK.[9,66] However, a subset of PCNSLs exhibits activating *CARD11* mutations in association with *MYD88*^{L265P} and *CD79B* mutations, which may limit the efficacy of proximal BCR pathway inhibitors.[9]

Recent studies highlight the complementary roles of BCR- and TLR-signaling in virus-driven B-cell activation, B-cell–intrinsic autoimmunity, and BCR-dependent survival.[60,61] In addition, both *MYD88*^{L265P} and *CARD11* mutations promote the breakdown of TLR and B-cell tolerance to self-antigens.[65,67] These observations are

	DLBCL		PTL	EBV⁻ PCNSL	PMBL
	All	ABC-type			
Genomic instability					
CDKN2A^{loss}	24% (43/180)[a]	35% (19/55)[a]	88% (44/50)[c]	71% (15/21)[k]	0% (0/11)
bi-alleic	19% (8/43)[a]	26% (5/19)[a]	77% (34/44)	73% (11/15)	0% (0/11)
CNAs of additional p53/cell cycle components	multiple [a,b]	multiple[a,b]	no	rare[d]	no
Total CNAs	high	high	high	high	low
Oncogenic TLR and BCR Signaling					
MYD88^{L265P}	12% (6/49)[e]	29% (45/155)[f]	78% (38/49)[g]	60% (33/55)[l]	NA
NFKBIZ^{gain}	9% (16/180)[a]	20% (11/55)[a]	42% (21/50)[h]	45% (28/62)[m]	0% (0/11)
NFKBIZ^{gain} and/or *MYD88*^{L265P}	NA	NA	92% (45/49)	83% (44/53)[n]	NA
CD79B^{Y196mut}					
Total	16% (8/49)[e]	23% (35/155)[f]	49% (22/45)[i]	38% (19/50)[o]	NA
Concurrent with *MYD88*^{L265P}	38% (3/8)[e]	43% (15/35)[f]	91% (20/22)	89% (17/19)	NA
PD-1 Ligand Deregulation					
9p24.1/*PD-L1*^{gain} and/or *PD-L2*^{gain}	6% (11/180)[a]	7% (4/55)[a]	54% (26/50)[h]	52% (33/63)[p]	55% (6/11)
PD-L1 or *PDL-2* translocation	NA	NA	4% (2/50)[j]	6% (4/66)[q]	20% (25/125)[r]

Figure 7. Unique combinations of structural alterations in discrete LBCL subtypes. Frequency of specific genetic alterations modulating "Genomic Instability," "Oncogenic TLR and BCR Signaling," and "PD-1 Ligand Deregulation" in DLBCL all, DLBCL ABC-type, PTL, EBV⁻ PCNSL, and PMBL are noted. a, Raw data previously published in reference 14. b, CNAs include the following alterations: *MDM2*^{gain}, *MDM4*^{gain}, *CDK2*^{gain}, *CDK4*^{gain}, *CDK6*^{gain}, *RB1*^{loss}, *RBL2*^{loss}, *TP53*^{loss}, *KDM6B*^{loss}, *RPL26*^{loss}, *BCL2L12*^{gain}, *RFWD2*^{gain}, *CCND3*^{gain}. c, *CDKN2A* CN data were available for 50 PTL (7 discovery + 43 extension). d, Only *RBL2*^{loss}. e, As reported in reference 54. f, As reported in reference 8. g, *MYD88*^{L265P} mutation status was available from 49 PTL (7 discovery + 42 extension). h, CN data for NFKBIZ and 9p24.1/PD-L1/PD-L2 loci were available from 50 PTL (7 discovery + 43 extension). i, *CD79B*^{Y196mut} mutation status in 45 PTL (7 discovery + 38 extension). j, 9p24.1/*PD-L1*/*PD-L2* translocation data were from 50 PTL (7 discovery + 43 extension). k, *CDKN2A* CN data were available for 21 EBV⁻ PCNSL (discovery only). l, *MYD88*^{L265P} mutation status was available from 55 EBV⁻ PCNSL (14 discovery + 41 extension). m, CN data for *NFKBIZ* locus were available from 62 EBV⁻ PCNSL (21 discovery + 41 extension). n, *NFKBIZ* CN data and *MYD88*^{L265P} mutation status were available for 53 EBV⁻ PCNSL (12 discovery + 41 extension). o, *CD79B*^{Y196mut} mutation status was available from 50 EBV⁻ PCNSL (12 discovery + 38 extension). p, 9p24.1/*PD-L1*/*PD-L2* CN data were from 63 EBV⁻ PCNSL (21 discovery + 42 extension). q, 9p24.1/*PD-L1*/*PD-L2* translocation data were from 66 EBV⁻ PCNSL (24 discovery + 42 extension). r, as reported in reference 19.

of note because candidate autoantigens were recently identified in PCNSL.[68,69]

Additional bases of tumor immune evasion in PTL and PCNSL—copy gain or translocation of *PD-L1* and/or *PD-L2*, and viral induction of PD-1 ligands

Our genetic analyses confirmed previously proposed mechanisms of tumor-immune escape: copy loss of 6p21.33 and the associated *HLA* loci, deletion of 15q21.1/*B2M*, and chromosomal rearrangement of *CIITA*.[18,24,25,70]

Strikingly, we also found 9p24.1 copy gain and increased expression of the PD-1 ligands in >50% of PTLs and EBV⁻ PCNSLs (Figure 7). In addition, we identified 4 EBV⁻ PCNSLs and 2 PTLs with chromosomal translocations that selectively deregulated *PD-L1* or *PD-L2*. In several tumors, proximal regulatory elements of other

genes (*TBL1XR1* and *BCNP1*) replaced the endogenous *PD-L1* or *PD-L2* promoter. In additional tumors, strong enhancer elements of *IgH* or *PAX5*[43] were juxtaposed to the intact endogenous *PD-L2* promoter. The *TBL1XR1-PD-L2* translocation both increased the expression of PD-L2 and inactivated *TBL1XR1*. Given the additional identified mutations in *TBL1XR1* (Figure 3 and supplemental Figure 6),[23,26,27] we postulate that *TBL1XR1* is a tumor suppressor in LBCLs.

Our combined genetic and IHC analyses suggest that tumors with discordant PD-L1 or PD-L2 expression and copy-neutral 9p24.1 status may harbor chromosomal rearrangements of *PD-L1* or *PD-L2*. The frequent genetic alterations of *PD-L2* also suggest that it may be preferable to target the PD-1 receptor rather than PD-L1.

Genetic alterations of 9p24.1 and associated overexpression of the PD-1 ligands have now been described in 4 lymphoid malignancies — cHL, PMBL, PTL, and PCNSL (Figure7,[16,19]). In EBV$^+$ PCNSL, as in other EBV$^+$ lymphoid malignancies, viral infection is an additional mechanism of PD-1 ligand overexpression.[62,63] The emerging data indicate that lymphoid malignancies with unique molecular signatures use common genetic mechanisms to increase the expression of PD-1 ligands (Figure 7). Given the demonstrated activity of PD-1 blockade in other lymphomas with 9p24.1 alterations,[22] this targeted therapy should also be considered in PTL and PCNSL. With respect to PCNSL, recent and ongoing clinical trials support the use of immunomodulatory antibodies in tumors involving the CNS[71] (www.clinicaltrials.gov, NCT02017717, NCT02311920, NCT02313272, NCT02311582).

Multiple genetic bases of target and pathway deregulation

Comprehensive analyses of CNAs, chromosomal rearrangements, and mutations revealed multiple mechanisms of target and pathway deregulation in PCNSL and PTL. For example, *ETV6* was altered by somatic mutations or exon deletion and *TBL1XR1* was perturbed by inactivating chromosomal translocations or somatic mutations. In addition, BCL6 was deregulated by mutations of *MEF2B*, chromosomal translocations of *BCL6* with immunoglobulin or nonimmunoglobulin regulatory elements, and a novel translocation of *PELI1*, which encodes an E3 ligase that stabilizes the BCL6 protein.[47]

Unique combinations of structural alterations in discrete LBCL subtypes

By comparing the comprehensive molecular signatures of PTL and PCNSL with those of systemic DLBCL and PMBLs, we identified unique combinations of genetic features in discrete LBCL subtypes (Figure 7). For example, PCNSLs, PTLs, and PMBLs exhibit frequent genetic alterations and overexpression of the PD-1 ligands,

whereas DLBCLs rarely have these features. Only a subset of transcriptionally defined ABC-type DLBCLs exhibit alterations of *MYD88* or *NFKBIZ*, whereas these are near-uniform genetic features of PCNSL and PTL. Although the majority of DLBCLs, PCNSLs, and PTLs exhibit increased genomic instability, as assessed by total CNAs, the genetic bases differ—multiple CNAs of p53/cell-cycle pathway components and *TP53* somatic mutations in DLBCL vs frequent, often biallelic, *CDKN2A* copy loss and rare *TP53* alterations in PCNSL and PTL (Figure 7).[14] In contrast, PMBLs have a paucity of CNAs.

Furthermore, the defining genetic features of PCNSL and PTL—near-uniform oncogenic TLR signaling, concurrent BCR activation, *CDKN2A* deficiency with wild-type p53, and PD-1–mediated immune evasion—suggest multiple targeted therapies that warrant clinical investigation.

Acknowledgements

This work was supported by National Institutes of Health, National Cancer Institute grant R01 CA161026 and an LLS Translational Research Award (M.A.S.), a Claudia Adams Barr Program in Basic Cancer Research (B.C.), National Institutes of Health, National Institute of Allergy and Infectious Diseases grant PO1 AI056299 (G.J.F.), and the Slim Initiative for Genomic Medicine, a project funded by the Carlos Slim Foundation in Mexico (Broad).

Authorship

Contribution: B.C. and M.G.M.R. designed research, performed research, analyzed data, and wrote the paper; C.S., Y.T., R.P.A., L.Z., A.J.D., M.D.D., D.G., G.G., and S.M. analyzed data; A.R.T., E.S.J., F.F., G.S.P., A.H.L., K.L.L., J.A.F., G.J.F., P.v.H., T.R.G., S.J.R., and D.d.J. performed research and analyzed data; D.M.M., G.L., G.I., E.A.L., H.H.S., H.H., and M.A. performed research; and M.A.S. designed research, analyzed data, and wrote the paper.

Conflict-of-interest disclosure: G.J.F. has patents and receives royalties on the PD-1 pathway from Amplimmune, Boehringer-Ingelheim, Bristol-Myers-Squibb (BMS), EDM-Serrono, Merck, Roche, and Novartis. M.A.S. has received research funding from BMS and served on advisory boards for BMS and Merck. The remaining authors declare no competing financial interests.

References

1. Rubenstein JL, Gupta NK, Mannis GN, Lamarre AK, Treseler P. How I treat CNS lymphomas. *Blood*. 2013;122(14):2318-2330.
2. Cheah CY, Wirth A, Seymour JF. Primary testicular lymphoma. *Blood*. 2014;123(4):486-493.
3. Horne MJ, Adeniran AJ. Primary diffuse large B-cell lymphoma of the testis. *Arch Pathol Lab Med*. 2011;135(10):1363-1367.
4. Deckert M, Montesinos-Rongen M, Brunn A, Siebert R. Systems biology of primary CNS lymphoma: from genetic aberrations to modeling in mice. *Acta Neuropathol*. 2014;127(2):175-188.
5. Riemersma SA, Jordanova ES, Schop RF, et al. Extensive genetic alterations of the HLA region, including homozygous deletions of HLA class II genes in B-cell lymphomas arising in immune-privileged sites. *Blood*. 2000;96(10):3569-3577.
6. Deng L, Xu-Monette ZY, Loghavi S, et al. Primary testicular diffuse large B-cell lymphoma displays distinct clinical and biological features for treatment failure in rituximab era: a report from the International PTL Consortium. *Leukemia*. 2016;30(2):361-372.
7. Basso K, Dalla-Favera R. Germinal centres and B cell lymphomagenesis. Nat Rev Immunol. 2015;15(3):172-184.
8. Ngo VN, Young RM, Schmitz R, et al. Oncogenically active MYD88 mutations in human lymphoma. *Nature*. 2011;470(7332):115-119.
9. Davis RE, Ngo VN, Lenz G, et al. Chronic active B-cell-receptor signalling in diffuse large B-cell lymphoma. *Nature*. 2010;463(7277):88-92.
10. Lenz G, Davis RE, Ngo VN, et al. Oncogenic CARD11 mutations in human diffuse large B cell lymphoma. *Science*. 2008;319(5870):1676-1679.
11. Monti S, Savage KJ, Kutok JL, et al. Molecular profiling of diffuse large B-cell lymphoma identifies robust subtypes including one characterized by host inflammatory response. *Blood*. 2005;105(5):1851-1861.
12. Caro P, Kishan AU, Norberg E, et al. Metabolic signatures uncover distinct targets in molecular subsets of diffuse large B cell lymphoma. *Cancer Cell*. 2012;22(4):547-560.
13. Chen L, Monti S, Juszczynski P, et al. SYK inhibition modulates distinct PI3K/AKT- dependent survival pathways and cholesterol biosynthesis in diffuse large B cell lymphomas. *Cancer Cell*. 2013;23(6):826-838.
14. Monti S, Chapuy B, Takeyama K, et al. Integrative analysis reveals an outcome-associated and targetable pattern of p53 and cell cycle deregulation in diffuse large B cell lymphoma. *Cancer Cell*. 2012;22(3):359-372.
15. Steidl C, Gascoyne RD. The molecular pathogenesis of primary mediastinal large B-cell lymphoma. *Blood*. 2011;118(10):2659-2669.
16. Green MR, Monti S, Rodig SJ, et al. Integrative analysis reveals selective 9p24.1 amplification, increased PD-1 ligand expression, and further induction via JAK2 in nodular sclerosing Hodgkin lymphoma and primary mediastinal large B-cell lymphoma. *Blood*. 2010;116(17):3268-3277.
17. Rui L, Emre NC, Kruhlak MJ, et al. Cooperative epigenetic modulation by cancer amplicon genes. *Cancer Cell*. 2010;18(6):590-605.
18. Steidl C, Shah SP, Woolcock BW, et al. MHC class II transactivator CIITA is a recurrent gene fusion partner in lymphoid cancers. *Nature*. 2011;471(7338):377-381.
19. Twa DD, Chan FC, Ben-Neriah S, et al. Genomic rearrangements involving programmed death ligands are recurrent in primary mediastinal large B-cell lymphoma. *Blood*. 2014;123(13):2062-2065.
20. Pardoll DM. The blockade of immune checkpoints in cancer immunotherapy. *Nat Rev Cancer*. 2012;12(4):252-264.
21. Keir ME, Butte MJ, Freeman GJ, Sharpe AH. PD-1 and its ligands in tolerance and immunity. *Annu Rev Immunol*. 2008;26:677-704.
22. Ansell SM, Lesokhin AM, Borrello I, et al. PD-1 blockade with nivolumab in relapsed or refractory Hodgkin's lymphoma. *N Engl J Med*. 2015;372(4):311-319.
23. Gonzalez-Aguilar A, Idbaih A, Boisselier B, et al. Recurrent mutations of MYD88 and TBL1XR1 in primary central nervous system lymphomas. *Clin Cancer Res*. 2012;18(19):5203-5211.
24. Braggio E, McPhail ER, Macon W, et al. Primary central nervous system lymphomas: a validation study of array-based comparative genomic hybridization in formalin-fixed paraffin-embedded tumor specimens. *Clin Cancer Res*. 2011;17(13):4245-4253.
25. Booman M, Szuhai K, Rosenwald A, et al. Genomic alterations and gene expression in primary diffuse large B-cell lymphomas of immune-privileged sites: the importance of apoptosis and immunomodulatory pathways. *J Pathol*. 2008;216(2):209-217.
26. Bruno A, Boisselier B, Labreche K, et al. Mutational analysis of primary central nervous system lymphoma. *Oncotarget*. 2014;5(13):5065-5075.
27. Vater I, Montesinos-Rongen M, Schlesner M, et al. The mutational pattern of primary lymphoma of the central nervous system determined by whole-exome sequencing. *Leukemia*. 2015;29(3):677-685.
28. Braggio E, Van Wier S, Ojha J, et al. Genome-Wide Analysis Uncovers Novel Recurrent Alterations in Primary Central Nervous System Lymphomas. *Clin Cancer Res*. 2015;21(17):3986-3994.
29. Kraan W, van Keimpema M, Horlings HM, et al. High prevalence of oncogenic MYD88 and CD79B mutations in primary testicular diffuse large B-cell lymphoma. *Leukemia*. 2014;28(3):719-720.
30. Oishi N, Kondo T, Nakazawa T, et al. High prevalence of the MYD88 mutation in testicular lymphoma: Immunohistochemical and genetic analyses. Pathol Int. 2015;65(10):528-535.
31. Beroukhim R, Getz G, Nghiemphu L, et al. Assessing the significance of chromosomal aberrations in cancer: methodology and application to glioma. Proc Natl Acad Sci U S A. 2007;104(50):20007-20012.

32. Nogai H, Wenzel SS, Hailfinger S, et al. IkappaB-zeta controls the constitutive NF-kappaB target gene network and survival of ABC DLBCL. *Blood*. 2013;122(13):2242-2250.
33. Yamamoto M, Yamazaki S, Uematsu S, et al. Regulation of Toll/IL-1-receptor-mediated gene expression by the inducible nuclear protein IkappaBzeta. *Nature*. 2004;430(6996):218-222.
34. Krappmann D. Shaping oncogenic NF-kappaB activity in the nucleus. Blood. 2013;122(13):2146-2147.
35. Hernando E, Nahle Z, Juan G, et al. Rb inactivation promotes genomic instability by uncoupling cell cycle progression from mitotic control. *Nature*. 2004;430(7001):797-802.
36. Wang L, He G, Zhang P, Wang X, Jiang M, Yu L. Interplay between MDM2, MDMX, Pirh2 and COP1: the negative regulators of p53. *Mol Biol Rep*. 2011;38(1):229-236.
37. Thompson SL, Compton DA. Proliferation of aneuploid human cells is limited by a p53-dependent mechanism. *J Cell Biol*. 2010;188(3):369-381.
38. Malumbres M, Barbacid M. Cell cycle, CDKs and cancer: a changing paradigm. *Nat Rev Cancer*. 2009;9(3):153-166.
39. Shlien A, Tabori U, Marshall CR, et al. Excessive genomic DNA copy number variation in the Li-Fraumeni cancer predisposition syndrome. *Proc Natl Acad Sci USA*. 2008;105(32):11264-11269.
40. Karras JR, Paisie CA, Huebner K. Replicative Stress and the FHIT Gene: Roles in Tumor Suppression, Genome Stability and Prevention of Carcinogenesis. *Cancers (Basel)*. 2014;6(2):1208-1219.
41. Drier Y, Lawrence MS, Carter SL, et al. Somatic rearrangements across cancer reveal classes of samples with distinct patterns of DNA breakage and rearrangement-induced hypermutability. *Genome Res*. 2013;23(2):228-235.
42. Abo RP, Ducar M, Garcia EP, et al. BreaKmer: detection of structural variation in targeted massively parallel sequencing data using kmers. *Nucleic Acids Res*. 2015;43(3):e19.
43. Chapuy B, McKeown MR, Lin CY, et al. Discovery and characterization of super-enhancer-associated dependencies in diffuse large B cell lymphoma. *Cancer Cell*. 2013;24(6):777-790.
44. Schneider C, Setty M, Holmes AB, et al. MicroRNA 28 controls cell proliferation and is down-regulated in B-cell lymphomas. *Proc Natl Acad Sci U S A*. 2014;111(22):8185-8190.
45. De Braekeleer E, Douet-Guilbert N, Morel F, Le Bris MJ, Basinko A, De Braekeleer M. ETV6 fusion genes in hematological malignancies: a review. *Leuk Res*. 2012;36(8):945-961.
46. Boyd RS, Adam PJ, Patel S, et al. Proteomic analysis of the cell-surface membrane in chronic lymphocytic leukemia: identification of two novel proteins, BCNP1 and MIG2B. *Leukemia*. 2003;17(8):1605-1612.
47. Park HY, Go H, Song HR, et al. Pellino 1 promotes lymphomagenesis by deregulating BCL6 polyubiquitination. *J Clin Invest.* 2014;124(11):4976-4988.
48. Tan Y, Chapuy B, Shipp M, Monti S. FusionQuery: a novel tool for gene-specific fusion detection. *International Conference on Intelligent Systems for Molecular Biology (ISMB)*; July 11-15, 2014, N06.
49. Lawrence MS, Stojanov P, Polak P, et al. Mutational heterogeneity in cancer and the search for new cancer-associated genes. *Nature*. 2013;499(7457):214-218.
50. De Silva NS, Simonetti G, Heise N, Klein U. The diverse roles of IRF4 in late germinal center B-cell differentiation. *Immunol Rev*. 2012;247(1):73-92.
51. Tijchon E, Havinga J, van Leeuwen FN, Scheijen B. B-lineage transcription factors and cooperating gene lesions required for leukemia development. *Leukemia*. 2013;27(3):541-552.
52. Huang W, Ghisletti S, Perissi V, Rosenfeld MG, Glass CK. Transcriptional integration of TLR2 and TLR4 signaling at the NCoR derepression checkpoint. *Mol Cell*. 2009;35(1):48-57.
53. Gil J, Peters G. Regulation of the INK4b-ARF-INK4a tumour suppressor locus: all for one or one for all. *Nat Rev Mol Cell Biol*. 2006;7(9):667-677.
54. Lohr JG, Stojanov P, Lawrence MS, et al. Discovery and prioritization of somatic mutations in diffuse large B-cell lymphoma (DLBCL) by whole-exome sequencing. *Proc Natl Acad Sci USA*. 2012;109(10):3879-3884.
55. Zhang J, Grubor V, Love CL, et al. Genetic heterogeneity of diffuse large B-cell lymphoma. *Proc Natl Acad Sci USA*. 2013;110(4):1398-1403.
56. Pasqualucci L, Trifonov V, Fabbri G, et al. Analysis of the coding genome of diffuse large B-cell lymphoma. *Nat Genet*. 2011;43(9):830-837.
57. Morin RD, Mendez-Lago M, Mungall AJ, et al. Frequent mutation of histone-modifying genes in non-Hodgkin lymphoma. *Nature*. 2011;476(7360):298-303.
58. Morin RD, Mungall K, Pleasance E, et al. Mutational and structural analysis of diffuse large B-cell lymphoma using whole-genome sequencing. *Blood*. 2013;122(7):1256-1265.
59. Ying CY, Dominguez-Sola D, Fabi M, et al. MEF2B mutations lead to deregulated expression of the oncogene BCL6 in diffuse large B cell lymphoma. *Nat Immunol*. 2013;14(10):1084-1092.
60. Jabara HH, McDonald DR, Janssen E, et al. DOCK8 functions as an adaptor that links TLR-MyD88 signaling to B cell activation. *Nat Immunol*. 2012;13(6):612-620.
61. Rawlings DJ, Schwartz MA, Jackson SW, Meyer-Bahlburg A. Integration of B cell responses through Toll-like receptors and antigen receptors. *Nat Rev Immunol*. 2012;12(4):282-294.
62. Green MR, Rodig S, Juszczynski P, et al. Constitutive AP-1 activity and EBV infection induce PD-L1 in Hodgkin lymphomas and posttransplant lymphoproliferative disorders: implications for targeted therapy. *Clin Cancer Res*. 2012;18(6):1611-1618.
63. Chen BJ, Chapuy B, Ouyang J, et al. PD-L1 expression is characteristic of a subset of aggressive B-cell lymphomas and virus-associated malignancies. *Clin Cancer Res*. 2013;19(13):3462-3473.
64. Chang YS, Graves B, Guerlavais V, et al. Stapled alpha-helical peptide drug development: a potent dual inhibitor of MDM2 and MDMX for p53-dependent cancer therapy. *Proc Natl Acad Sci USA*. 2013;110(36):E3445-3454.

65. Wang JQ, Jeelall YS, Beutler B, Horikawa K, Goodnow CC. Consequences of the recurrent MYD88(L265P) somatic mutation for B cell tolerance. *J Exp Med*. 2014;211(3):413-426.
66. Yang Y, Shaffer AL, 3rd, Emre NC, et al. Exploiting synthetic lethality for the therapy of ABC diffuse large B cell lymphoma. *Cancer Cell*. 2012;21(6):723-737.
67. Jeelall YS, Wang JQ, Law HD, et al. Human lymphoma mutations reveal CARD11 as the switch between self-antigen-induced B cell death or proliferation and autoantibody production. *J Exp Med*. 2012;209(11):1907-1917.
68. Thurner L, Kemele M, Fadle N, et al. Postranslationally modified proteins in the central nervous system (CNS) are the dominant antigenic target/stimulus of the B-cell receptor (BCR) in primary CNS lymphomas (PCNSL) providing strong evidence for the role of chronic autoantigenic stimulation as an early step in the pathogenesis of aggressive B-cell lymphomas [abstract]. *Blood*. 2014;124(21). Abstract 142.
69. Trepel M, Muller F, Illerhaus G, Glatzel M, Binder M, Spier E. B-cell receptors of primary central nervous system lymphoma recognize antigens in the brain [abstract]. *Blood*. 2014;124(21). Abstract 3003.
70. Green MR, Kihira S, Liu CL, et al. Mutations in early follicular lymphoma progenitors are associated with suppressed antigen presentation. *Proc Natl Acad Sci USA*. 2015;112(10):E1116-1125.
71. Margolin K, Ernstoff MS, Hamid O, et al. Ipilimumab in patients with melanoma and brain metastases: an open-label, phase 2 trial. *Lancet Oncol*. 2012;13(5):459-465.